

High-powered Microwave Ablation with a Small-gauge, Gas-cooled Antenna: Initial Ex Vivo and In Vivo Results

Meghan G. Lubner, MD, J. Louis Hinshaw, MD, Anita Andreano, MD, Lisa Sampson, BS, Fred T. Lee, Jr, MD, and Christopher L. Brace, PhD

ABSTRACT

Purpose: To evaluate the performance of a gas-cooled, high-powered microwave system.

Materials and Methods: Investigators performed 54 ablations in ex vivo bovine livers using three devices—a single 17-gauge cooled radiofrequency (RF) electrode; a cluster RF electrode; and a single 17-gauge, gas-cooled microwave (MW) antenna—at three time points (n = 6 at 4 minutes, 12 minutes, and 16 minutes). RF power was applied using impedance-based pulsing with maximum 200 W generator output. MW power of 135 W at 2.45 GHz was delivered continuously. An approved in vivo study was performed using 13 domestic pigs. Hepatic ablations were performed using single applicators and the above-mentioned MW and RF generator systems at treatment times of 2 minutes (n = 7 MW, n = 6 RF), 5 minutes (n = 23 MW, n = 8 RF), 7 minutes (n = 11 MW, n = 6 RF), and 10 minutes (n = 7 MW, n = 9 RF). Mean transverse diameter and length of the ablation zones were compared using analysis of variance (ANOVA) with post-hoc *t* tests and Wilcoxon rank-sum tests.

Results: Single ex vivo MW ablations were larger than single RF ablations at all time points (MW mean diameter range 3.5–4.8 cm 4–16 minutes; RF mean diameter range 2.6–3.1 cm 4–16 minutes) ($P < .05$). There was no difference in mean diameter between cluster RF and MW ablations (RF 3.3–4.4 cm 4–16 minutes; $P = .4$ –.9). In vivo lesion diameters for MW (and RF) were as follows: 2.6 cm \pm 0.72 (RF 1.5 cm \pm 0.14), 3.6 cm \pm 0.89 (RF 2.0 cm \pm 0.4), 3.4 cm \pm 0.87 (RF 1.8 cm \pm 0.23), and 3.8 cm \pm 0.74 (RF 2.1 cm \pm 0.3) at 2 minutes, 5 minutes, 7 minutes, and 10 minutes ($P < .05$ all time points).

Conclusions: Gas-cooled, high-powered MW ablation allows the generation of large ablation zones in short times.

ABBREVIATIONS

ANOVA = analysis of variance, MW = microwave, RF = radiofrequency, SAD = short axis diameter

Although radiofrequency (RF) ablation accounts for many of the clinical and experimental studies in heat-based ablation to date, RF power delivery is limited by desiccation in the ablation zone and water vaporization as temperatures approach 100°C. Slower heating protocols and power-switching techniques that are used to compensate for limited power delivery result in slow heating, long ablation times, and small ablation zones. As a result, RF is often

inadequate to treat many tumors encountered in clinical practice when using a single applicator (1–3). In recent years, attention has begun to focus on microwave (MW) ablation as an alternative ablation modality (4–9).

MW tissue heating relies on the oscillation of polar molecules such as water and does not depend on the conduction of electricity (10–17). As a result of this mechanistic difference in heating, MW ablation has many theo-

From the Department of Radiology (M.G.L., J.L.H., L.S., F.T.L., C.L.B.), University of Wisconsin School of Medicine and Public Health, E3/311 Clinical Sciences Center, 600 Highland Avenue, Madison, WI 53792-3252; Departments of Biomedical Engineering (C.L.B.) and Medical Physics (C.L.B.), University of Wisconsin, Madison, Wisconsin; and Department of Radiology (A.A.), University of Milan, Milan, Italy. Received August 11, 2011; final revision received November 1, 2011; accepted November 6, 2011. Address correspondence to M.G.L.; E-mail: mlubner@uwhealth.org

Preliminary data presented at World Conference on Interventional Oncology, June 2010.

J.L.H. is a stockholder of NeuWave Medical (Madison, WI). L.S. is a consul-

tant for NeuWave Medical. F.T.L. is a stockholder for and serves on the board of directors of NeuWave Medical. C.L.B. is a stockholder of and consultant for NeuWave Medical. Neither of the other authors has identified a conflict of interest.

NIH funding (1 R01 CA142737-01, L30 CA136262-01) was received to support ablation research.

© SIR, 2012

J Vasc Interv Radiol 2012; 23:405–411

DOI: 10.1016/j.jvir.2011.11.003

retical advantages over RF ablation. MWs are capable of effectively heating many tissue types, even tissues with high impedance such as lung and bone (12). MWs can also penetrate charred or desiccated tissues, allowing continuous power application for the duration of the treatment, generation of very high temperatures, and less susceptibility to heat sink effects (14,18–21).

Commercial MW systems have been hampered by antenna shaft heating during high-power application, which can cause thermal damage to the skin and lead to potentially serious complications such as fistula (22). Possible solutions include limiting power output, increasing antenna diameter to reduce shaft heating, or active cooling of the antenna shaft. Reducing power output results in smaller ablations, and large-diameter antennas may be unsuitable for percutaneous use (15). Active cooling with water circulation has been shown to allow increased power delivery while reducing shaft heating. However, the viscosity of water can limit flow and cooling capacity in small-diameter antennas (8,15,23–27). Another strategy for cooling is the use of compressed gas. A high-power, gas-cooled MW system was introduced more recently that uses carbon dioxide as a cooling refrigerant (4). The cooling capacity of this system allows the application of high-power generators (140 W), while maintaining small antenna diameters (17-gauge). The objective of this study was to evaluate and compare the performance of this gas-cooled MW system with an existing cooled RF device in ex vivo bovine livers and in vivo porcine livers.

MATERIALS AND METHODS

Approval for our study was obtained from our institutional research animal care and use committee. All husbandry and experimental studies were compliant with the National Institutes of Health *Guide for the Care and Use of Laboratory Animals* (<http://oacu.od.nih.gov/regs/guide/guidex.htm>).

Ex Vivo Methods

We performed 54 ablations in six ex vivo bovine livers. Three devices—a single 17-gauge cooled RF electrode (Cool-tip; Covidien, Boulder, Colorado), a cluster RF electrode (Cool-tip cluster; Covidien), and a single 17-gauge gas-cooled MW antenna (Certus 140; NeuWave Medical, Madison, Wisconsin)—were evaluated. For each device, three ablation times were used (4, 12, and 16 minutes), with six ablations performed in each group. RF power was delivered using an impedance-based pulsing algorithm with a maximum 200 W generator output. Cooling water was maintained at approximately 4°C and circulated at a rate of 40 mL/min. The MW power was delivered continuously with a generator output of 135 W at 2.45 GHz. Zones of coagulation were excised en bloc and sectioned transverse to the ablation applicator into approximately 5-mm slices. Maximum, minimum, and mean diameters; length; area; and circularity of each ablation zone were measured. Com-

Table 1. Ablation Results in Ex Vivo Bovine Liver Using Three Different Ablation Devices*

	Single RF (cm)	Cluster RF (cm)	Single MW (cm)
4 min	2.6 ± 0.1	3.3 ± 0.2	3.5 ± 0.2
12 min	3.2 ± 0.3	4.4 ± 0.3	4.7 ± 0.4
16 min	3.1 ± 0.3	4.4 ± 0.2	4.8 ± 0.2

MW = microwave; RF = radiofrequency.

* n = 6 for each cell.

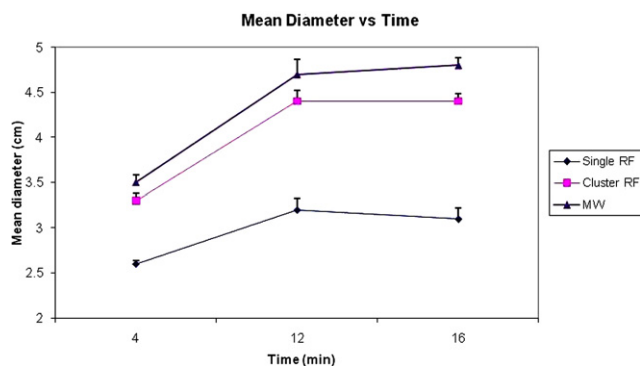


Figure 1. Graph shows the change in mean ablation diameter over time by the ablation device in an ex vivo bovine liver. MW ablations (triangles) are larger than single RF ablations (diamonds) at each time point. There was no statistical difference between MW ablations and cluster RF ablations (squares). Error bars represent standard error of the mean. (Available in color online at www.jvir.org.)

parison between groups was performed using analysis of variance (ANOVA) and post-hoc *t* tests.

In Vivo Methods

Animals, Anesthesia, and Overview of Procedures. We used 13 female domestic swines (Arlington Farms, Arlington, Wisconsin) (mean weight 45 kg) for this study. Ketamine was administered for preanesthetic sedation. Sedated animals were intubated, and anesthesia was maintained with inhaled isoflurane (Halocarbon Laboratories, River Edge, New Jersey). The liver was surgically exposed at laparotomy with a bilateral subcostal incision to enable applicator placement and to verify proper positioning. Either RF or MW ablation was performed in each of four distinct liver lobes, and different ablation times were distributed among the animals. After ablation, the animals were euthanized with an overdose of pentobarbital sodium and phenytoin sodium (Beuthanasia-D; Schering-Plough, Kenilworth, New Jersey). Zones of ablation were excised and sectioned as described subsequently.

Microwave Ablations. We performed 48 MW ablations. All MW ablations were performed using a 17-gauge gas-cooled triaxial antenna (Certus 140, LK 15; NeuWave Medical) tuned for liver tissue. This antenna has an emission point located 2 cm back from the tip that constitutes the active zone. MW power was applied continuously at 140 W from the

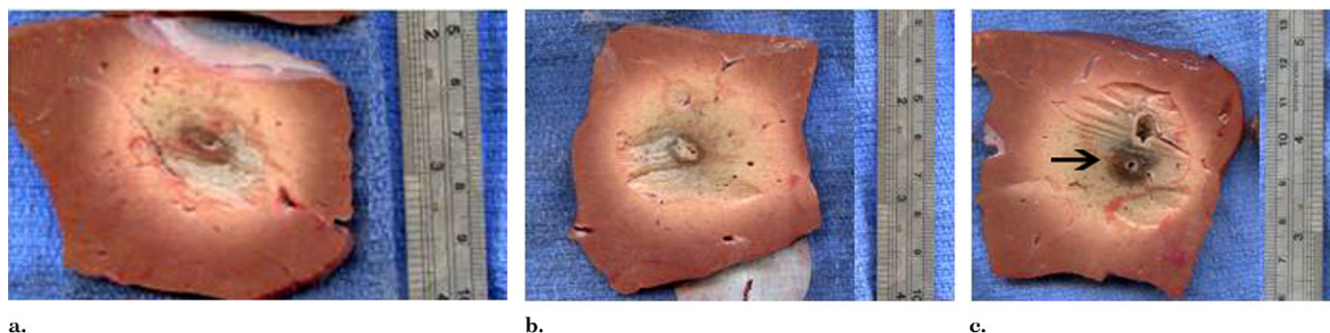


Figure 2. Gross sections of ex vivo ablation zones. Sections perpendicular to the applicator were obtained using a single RF probe (a, 3.0 × 4.0 cm), cluster RF probe (b, 3.8 × 4.8 cm), and MW antenna (c, 4.3 × 4.5 cm) for 12 minutes. Note the denser inner char seen in the MW ablation zone (arrow in c). (Available in color online at www.jvir.org.)

Table 2. Mean Ablation Zone Diameter in In Vivo Porcine Liver Using Two Different Ablation Devices

	Single RF (cm)	Single MW (cm)	P Value
2 min	1.5 ± 0.1	2.6 ± 0.7	.001
5 min	2.0 ± 0.4	3.6 ± 0.89	3.0 × 10 ⁶
7 min	1.8 ± 0.2	3.4 ± 0.9	.0003
10 min	2.1 ± 0.3	3.8 ± 0.7	.0003

MW = microwave; RF = radiofrequency.

2.45-GHz solid-state generator for 2 minutes (n = 7), 5 minutes (n = 23), 7 minutes (n = 11), and 10 minutes (n = 7). These shorter time periods were selected based on growth trends observed in the ex vivo data. We performed at least one ablation in each lobe of each porcine liver.

Radiofrequency Ablations. All RF ablations were performed using a single 17-gauge water-cooled electrode as in the ex vivo studies. Applicators with 3-cm active zones were used. Ablation times of 2 minutes (n = 6), 5 minutes (n = 8), 7 minutes (n = 6), and 10 minutes (n = 9) were used for comparison with the MW groups. The cluster probe evaluated in the ex vivo portion was not used in the in vivo study.

Measurements of Ablation Zone Size and Shape. Ablation zones were sliced, measured, and scanned according to our previously presented methods (14), which include optical scanning of ablation zones (Perfection 2450 Photograph, model G860A; Epson, Long Beach, California) that were saved as electronic images. For each ablation zone, a representative slice near the middle of each ablation zone was chosen for measurement. Standard ablation zone metrics including maximum and minimum diameter and circularity (as an isoperimetric ratio) were analyzed using free software (ImageJ; National Institutes of Health, Bethesda, Maryland) (14,25). Most samples were sectioned perpendicular to the length of the ablation applicator. In four of the in vivo samples, we elected to slice the ablation zone along the antenna axis. In these cases, only a single transverse diameter could be evaluated. We included this transverse diameter measurement into the mean diameter dataset for statistical analysis. Mean diameter was calculated as the

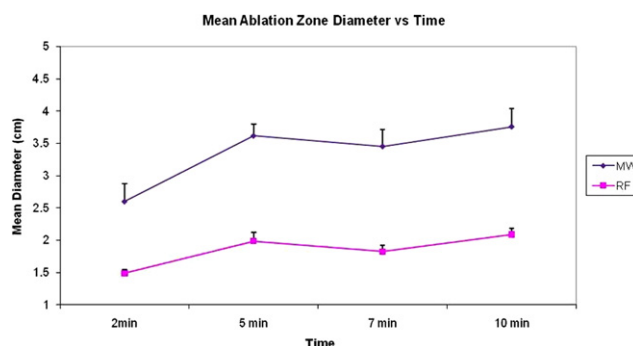


Figure 3. Graph shows mean diameter of the ablation zone over time by the ablation device in an in vivo porcine liver. As seen with the ex vivo data, MW ablations (diamonds) were significantly larger than RF ablations (squares) at all time points. Error bars represent standard error of the mean. (Available in color online at www.jvir.org.)

average of the minimum and maximum diameter, or the transverse diameter was used, as available.

Statistical Analysis

Descriptive statistics of each metric (mean diameter, length, area, circularity) was calculated at each time point for both MW and RF ablations. Comparison between ex vivo groups was performed using ANOVA and post-hoc *t* tests. In vivo data were analyzed using a Wilcoxon rank-sum test because the data were not normally distributed. The analysis did not account for clustering of lobes within animals because lobes were considered as independent. Exploratory analyses were obtained to assess the validity of statistical test assumptions. A *P* value < .05 was considered to indicate a significant difference. Statistical analyses were performed in R2.12.1 (28).

RESULTS

Ex Vivo Results

Ablation zones created with a single MW antenna had larger minimum, maximum, and mean diameters than ablation zones produced by a single RF electrode at all time points in the ex

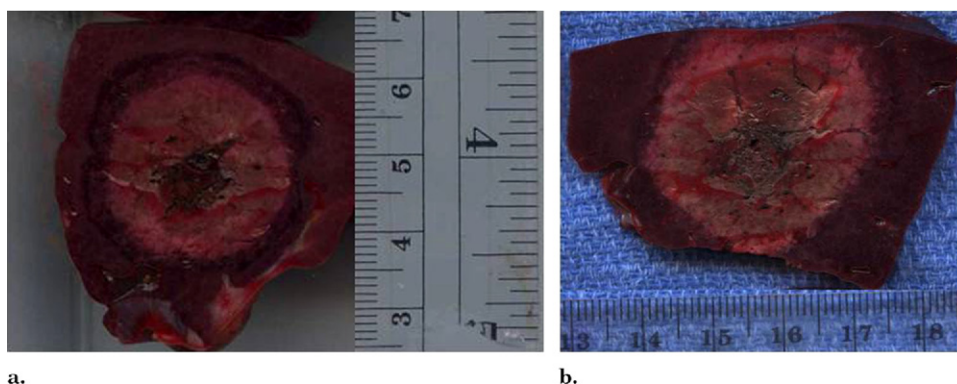


Figure 4. Two gross sections obtained perpendicular to the applicators from an in vivo porcine liver. A representative ablation zone created using RF for 10 minutes (a), measuring 2.4×2.5 cm, is smaller than the ablation zone seen with MW (b), measuring 3.3×3.8 cm. The MW ablation zone rose to the liver surface, which may constrain the size of the ablation zone. (Available in color online at www.jvir.org.)

Table 3. Minimum and Maximum Diameter and Circularity in In Vivo Porcine Liver Using Two Different Ablation Devices

	RF Minimum Diameter (cm)	MW Minimum Diameter (cm)	RF Maximum Diameter (cm)	MW Maximum Diameter (cm)	RF Circularity	MW Circularity
2 min	1.4 ± 0.17	2.0 ± 0.23	1.6 ± 0.13	3.2 ± 1.2	0.94 ± 0.14	0.86 ± 0.08
5 min	1.8 ± 0.35	2.6 ± 0.66	2.2 ± 0.40	4.9 ± 1.3	0.90 ± 0.02	0.74 ± 0.15
7 min	1.65 ± 0.26	2.1 ± 0.26	2.0 ± 0.26	5.4 ± 1.1	0.92 ± 0.03	0.65 ± 0.09
10 min	1.8 ± 0.28	3.4 ± 0.60	2.4 ± 0.39	4.1 ± 0.9	0.90 ± 0.05	0.84 ± 0.19

MW = microwave; RF = radiofrequency.

vivo bovine liver model ($P < .05$). There was no difference in the size of ablations created using the MW system and the RF cluster electrode ($P = .4$ – $.9$) (Table 1, Figures 1 and 2). All ablation zones were highly circular with no significant differences noted in the isoperimetric ratio between any groups (range for all groups 0.95–0.98). Qualitatively, the MW ablation zones were round, without any obvious tails along the antenna shaft. Both RF and MW ablations contained dense inner zones immediately surrounding the applicator, although this central zone was thicker and darker in MW ablations (Figure 2).

In Vivo Results

In the in vivo porcine normal liver model, single MW ablations were significantly larger than single RF ablations at all time points ($P < .001$ for all time points) (Table 2, Figures 3 and 4); this held true for mean, minimum, and maximum diameters (Table 3). MW ablation zones were longer than RF ablation zones, measuring $5.3 \text{ cm} \pm 0.2$ at 5 minutes and $5.8 \text{ cm} \pm 0.3$ at 10 minutes (RF $4.2 \text{ cm} \pm 0.2$ and $4.0 \text{ cm} \pm 0.7$). However, because the MW ablations were larger in diameter, the ratio of diameter to length was greater for MW ablations at both time points (MW 0.66 and 0.70; RF 0.48 and 0.53). The ablation zone with MW was well seen on ultrasound images, with hyperechoic gas bubbles generated during power delivery that were similar in appearance to RF ablation. The gas was noted to clear rapidly (1–2 minutes), leaving a hypoechoic ablation zone with a slightly hyperechoic halo.

MW ablation zones showed significant growth from 2 minutes to 5 minutes ($P = .003$) and when comparing 2-minute ablations with time points beyond 5 minutes (2 min vs 7 min, $P = .011$; 2 min vs 10 min, $P = .038$). However, there was no significant difference in ablation zone size when comparing 5 minutes vs 7 minutes ($P = .76$) or 5 minutes vs 10 minutes ($P = .92$). A similar trend was seen with the RF ablation zones (2 min vs 5 min, $P = .004$; 5 min vs 7 min, $P = .75$; 5 min vs 10 min, $P = .43$).

DISCUSSION

The results of our study show that gas-cooled, small-diameter MW antennas consistently create large ablation zones in relatively short time periods. Ablations were significantly larger at all time points compared with water-cooled RF ablation with a single electrode. The RF ablation zones seen in this study are similar to or larger in size than the zones seen in other published in vivo series using similar models. Laeseke et al (29) obtained a mean diameter of 1.6 cm at 12 minutes using a single water-cooled RF probe. The size of the MW ablation zones reported in this study (3.7 cm at 5 minutes, 3.8 cm at 10 minutes) are much larger than other in vivo experiments (Table 4). Hope et al (30) generated ablation zones using a water-cooled 14-gauge antenna in a similar in vivo porcine model with a 915-MHz generator at 45 W with mean diameter of $2.0 \text{ cm} \pm 2.4$ at 10 minutes. Wright et al (31) obtained a mean diameter of 2.1 cm using

Table 4. Prior Microwave and Radiofrequency In Vivo Results

Study, Year	Model	System	Ablation Zone Size
Laeseke et al (29), 2006	In vivo porcine	Water-cooled RF, 17-gauge, 200 W, impedance-based pulsing	Mean diameter 12 min—1.6 cm
Wright et al (31), 2005	In vivo porcine	915 MHz, 40 W, 13-gauge, 10 min, water cooling	Mean diameter 10 min—2.1 cm
Brace et al (14), 2007	In vivo porcine	2.45 GHz, 68 W, 17-gauge, 12 min, water cooling	Mean diameter 2 min—2.3 cm 6 min—2.6 cm 12 min—2.9 cm
Awad et al (21), 2007	In vivo porcine	2.45 GHz, 100 W, 5.7 mm, 2–8 min	Mean volume 2 min—33.5 cm ³ 4 min—37.5 cm ³ 8 min—92 cm ³
Hines-Peralta et al (15), 2006	Ex vivo bovine, in vivo porcine	2.45 GHz, 50–150 W, 5.7 mm, 2–20 min	Ex vivo SAD 4.9 cm In vivo SAD 5.7 cm
Iannitti et al (7), 2007	Clinical	915 MHz, 45 W, 14-gauge, 10 min	Mean volume 10 cm ³
Hope et al (30), 2008	In vivo porcine	915 MHz, 45 W, 14-gauge, 10 min	Mean diameter 2.0 ± 2.4 cm

RF = radiofrequency, SAD = short axis diameter.

a 13-gauge water-cooled device using 40 W at 915 MHz. In a separate study, Brace et al (14) used an uncooled 17-gauge antenna to generate ablation zones of 2.9 cm at 12 minutes using 68 W at 2.45 GHz. The large thermal lesions reported in our study are likely a result of the high powers possible with this particular gas-cooled system.

The significant increase in size in MW ablation zones between time points of 2 minutes and longer may be due to the rapid generation of very high temperatures and the decreased impact of charring and desiccation on MW heating compared with RF. However, growth of the mean diameter of the ablation zone slowed after 5 minutes in this data set. Beyond this time point, the ablation zones became slightly more circular (circularity at 5 minutes 0.73, circularity at 10 minutes 0.84), but there was not much gain in mean diameter with a single probe. A confounding factor is tissue contraction at high temperatures, which is greater for MW than RF because of higher tissue temperatures and which appears to increase as ablation time progresses (32). Contraction owing to water vaporization and tissue desiccation causes the excised specimen to appear smaller than the original (ie, preablation) tissue dimensions. Although thermal energy may continue to progress radially outward at later time points, such gains may be offset by tissue contraction.

As seen when comparing the ex vivo and in vivo MW data (Figure 5), the ablation zone sizes are similar in the first few minutes, but as time progresses the in vivo ablation zones do not continue to grow as much as the ex vivo ablation zones. This effect is not seen with RF (Figure 6), where all ex vivo ablation zones are larger than in vivo

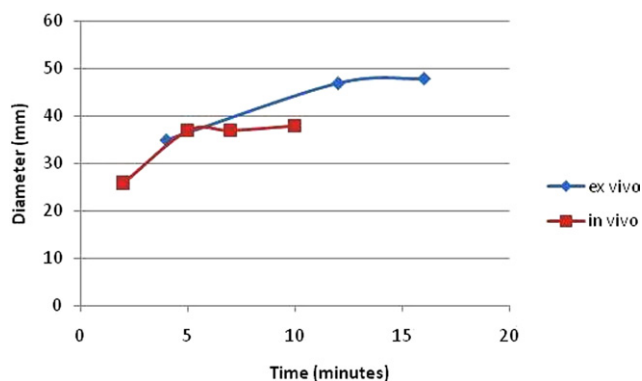


Figure 5. Graph comparing the ex vivo (bovine) and in vivo (porcine) mean MW ablation zone diameters over time. At early time points, the ablation zone sizes are similar between the models, with the in vivo ablation zones smaller at later time points, possibly related partly to tissue contraction and greater reliance on thermal conduction later in the ablation. (Available in color online at www.jvir.org.)

ablation zones. This trend was also observed in a previous MW ablation study (15). A possible explanation might be that direct MW heating dominates any positive heat flux from thermal diffusion or negative heat flux caused by blood perfusion during the first few minutes. At later time points, an equilibrium is set up at the front between positive heat flux from thermal diffusion and negative heat flux from blood perfusion—that is, ablation zone expansion is effectively counteracted by blood perfusion at the ablation zone boundary (33,34). This equilibrium may also help explain the lack of ablation zone growth after 5 minutes in vivo. In addition, the porcine hepatic lobes are thinner than hepatic

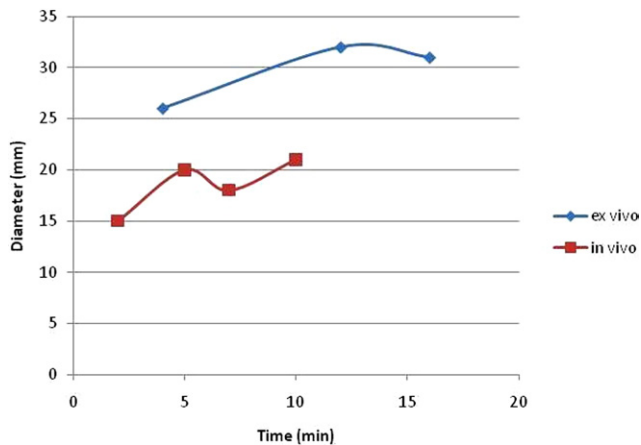


Figure 6. Graph comparing the ex vivo (bovine) and in vivo (porcine) mean RF ablation zone diameters over time. All ex vivo ablation zones are larger than the in vivo ablation zones, in contradistinction to the data seen for MW in **Figure 5**. (Available in color online at www.jvir.org.)

lobes in humans, so the MW ablations were constrained by the tissue surface, especially at longer time points.

Although MW ablations were longer than RF ablations, we noted that the MW ablations were more spherical overall. The greater length was related to the greater overall size of the ablation. However, when working adjacent to vulnerable structures, at the surface of an organ, or treating patients with small tumors, this added length may be problematic. A more precise applicator or technique may be needed to generate a shorter ablation zone for some indications, or adjunctive techniques such as hydrodissection may need to be aggressively used. In addition, given that large ablation zones can be achieved over short times with this device, further characterization is likely to be required at various power and time settings to provide users with an appropriate range of target ablation sizes.

Limitations of this study include the exclusive use of normal porcine liver rather than a tumor model or cirrhotic liver. More recent data using a water-cooled 2.45-GHz system at 100 W (Amica; HS Medical, Boca Raton, Florida) suggest that the performance in human tumors can be expected to be somewhere between the performance seen in ex vivo and in vivo normal porcine livers (35). An additional limitation was that the in vivo portion of this study was performed using an open approach to minimize variations in applicator positioning and to maximize the number of ablations per animal and reduce the total number of animals sacrificed for the study. Because this small-caliber, gas-cooled antenna was specifically designed for percutaneous use, further study in percutaneous and clinical models seems warranted. Some additional characterization of time and power curves for single applicators and multi-antenna assessment is also likely needed to guide clinical application.

In conclusion, the gas-cooled MW ablation system evaluated in this study is able to generate large ablation

zones in short times with a small-gauge, minimally invasive applicator. Further evaluation of this system in a clinical setting is warranted. Further study with multiprobe ablation is needed, and further development of a more precise probe with a shorter ablation zone may be helpful for treating smaller tumors.

REFERENCES

- Kim YS, Rhim H, Cho OK, Koh BH, Kim Y. Intrahepatic recurrence after percutaneous radiofrequency ablation of hepatocellular carcinoma: analysis of the pattern and risk factors. *Eur J Radiol* 2006; 59:432–441.
- Livraghi T, Goldberg SN, Lazzaroni S, et al. Hepatocellular carcinoma: radio-frequency ablation of medium and large lesions. *Radiology* 2000; 214:761–768.
- Lu DS, Raman SS, Limanond P, et al. Influence of large peritumoral vessels on outcome of radiofrequency ablation of liver tumors. *J Vasc Interv Radiol* 2003; 14:1267–1274.
- Lubner MG, Brace CL, Hinshaw JL, Lee FT Jr. Microwave tumor ablation: mechanism of action, clinical results, and devices. *J Vasc Interv Radiol* 2010; 21:S192–S203.
- Dong B, Liang P, Yu X, et al. Percutaneous sonographically guided microwave coagulation therapy for hepatocellular carcinoma: results in 234 patients. *AJR Am J Roentgenol* 2003; 180:1547–1555.
- Castle SM, Salas N, Leveillee RJ. Initial experience using microwave ablation therapy for renal tumor treatment: 18-month follow-up. *Urology* 2011; 77:792–797.
- Iannitti DA, Martin RC, Simon CJ, et al. Hepatic tumor ablation with clustered microwave antennae: the US Phase II Trial. *HPB (Oxford)* 2007; 9:120–124.
- Kuang M, Lu MD, Xie XY, et al. Liver cancer: increased microwave delivery to ablation zone with cooled-shaft antenna—experimental and clinical studies. *Radiology* 2007; 242:914–924.
- Liang P, Wang Y. Microwave ablation of hepatocellular carcinoma. *Oncology* 2007; 72:124–131.
- Brace CL. Microwave ablation technology: what every user should know. *Curr Probl Diagn Radiol* 2009; 38:61–67.
- Duck F. *Physical Properties of Tissue: A Comprehensive Reference Book*. London: Academic Press; 1990.
- Brace CL. Radiofrequency and microwave ablation of the liver, lung, kidney, and bone: what are the differences? *Curr Probl Diagn Radiol* 2009; 38:135–143.
- Simon CJ, Dupuy DE, Mayo-Smith WW. Microwave ablation: principles and applications. *Radiographics* 2005; 25:S69–S83.
- Brace CL, Laeseke PF, Sampson LA, et al. Microwave ablation with a single small-gauge triaxial antenna: in vivo porcine liver model. *Radiology* 2007; 242:435–440.
- Hines-Peralta AU, Pirani N, Clegg P, et al. Microwave ablation: results with a 2.45-GHz applicator in ex vivo bovine and in vivo porcine liver. *Radiology* 2006; 239:94–102.
- Shock SA, Meredith K, Warner TF, et al. Microwave ablation with loop antenna: in vivo porcine liver model. *Radiology* 2004; 231:143–149.
- Lu MD, Xu HX, Xie XY, et al. Percutaneous microwave and radiofrequency ablation for hepatocellular carcinoma: a retrospective comparative study. *J Gastroenterol* 2005; 40:1054–1060.
- Yang D, Converse MC, Mahvi DM, Webster JG. Measurement and analysis of tissue temperature during microwave liver ablation. *IEEE Trans Biomed Eng* 2007; 54:150–155.
- Bhardwaj N, Strickland AD, Ahmad F, Atanesyan L, West K, Lloyd DM. A comparative histological evaluation of the ablations produced by microwave, cryotherapy and radiofrequency in the liver. *Pathology (Phila)* 2009; 41:168–172.
- Yu NC, Raman SS, Kim YJ, Lassman C, Chang X, Lu DS. Microwave liver ablation: influence of hepatic vein size on heat-sink effect in a porcine model. *J Vasc Interv Radiol* 2008; 19:1087–1092.
- Awad MM, Devgan L, Kamel IR, Torbensen M, Choti MA. Microwave ablation in a hepatic porcine model: correlation of CT and histopathologic findings. *HPB (Oxford)* 2007; 9:357–362.
- Liang P, Wang Y, Yu X, Dong B. Malignant liver tumors: treatment with percutaneous microwave ablation—complications among cohort of 1136 patients. *Radiology* 2009; 251:933–940.

23. Wolf FJ, Grand DJ, Machan JT, Dipetrillo TA, Mayo-Smith WW, Dupuy DE. Microwave ablation of lung malignancies: effectiveness, CT findings, and safety in 50 patients. *Radiology* 2008; 247:871–879.
24. Strickland AD, Clegg PJ, Cronin NJ, et al. Experimental study of large-volume microwave ablation in the liver. *Br J Surg* 2002; 89:1003–1007.
25. Brace CL, Laeseke PF, van der Weide DW, Lee FT. Microwave ablation with a triaxial antenna: results in ex vivo bovine liver. *IEEE Trans Microw Theory Tech* 2005; 53:215–220.
26. Shibata T, Jimuro Y, Yamamoto Y, et al. Small hepatocellular carcinoma: comparison of radio-frequency ablation and percutaneous microwave coagulation therapy. *Radiology* 2002; 223:331–337.
27. Wang Y, Sun Y, Feng L, Gao Y, Ni X, Liang P. Internally cooled antenna for microwave ablation: results in ex vivo and in vivo porcine livers. *Eur J Radiol* 2008; 67:357–361.
28. RDCT. R: A language and environment for statistical computing. R Foundation for Statistical Computing. 2009. Available at: <http://www.R-project.org>. Accessed July 2011.
29. Laeseke PF, Sampson LA, Haemmerich D, et al. Multiple-electrode radiofrequency ablation creates confluent areas of necrosis: in vivo porcine liver results. *Radiology* 2006; 241:116–124.
30. Hope WW, Schmelzer TM, Newcomb WL, et al. Guidelines for power and time variables for microwave ablation in a porcine liver. *J Gastrointest Surg* 2008; 12:463–467.
31. Wright AS, Sampson LA, Warner TF, Mahvi DM, Lee FT Jr. Radiofrequency versus microwave ablation in a hepatic porcine model. *Radiology* 2005; 236:132–139.
32. Brace CL, Diaz TA, Hinshaw JL, Lee FT Jr. Tissue contraction caused by radiofrequency and microwave ablation: a laboratory study in liver and lung. *J Vasc Interv Radiol* 2010; 21:1280–1286.
33. Schramm W, Yang D, Haemmerich D. Contribution of direct heating, thermal conduction and perfusion during radiofrequency and microwave ablation. *Conf Proc IEEE Eng Med Biol Soc* 2006; 1:5013–5016.
34. Schramm W, Yang D, Wood BJ, Rattay F, Haemmerich D. Contribution of direct heating, thermal conduction and perfusion during radiofrequency and microwave ablation. *Open Biomed Eng J* 2007; 1:47–52.
35. Goldberg SN, Meloni F, Tosoratti N, Nissenbaum I, Appelbaum L, Solbiati L. Parameter characterization for microwave tumor ablation: comparison of experimental and HCC data. Paper presented at: World Conference on Interventional Oncology; June 2011; New York.